Stress Measurement in MEMS Devices

L. Starman, Jr.*, J. Busbee**, J. Reber**, J. Lott*, W. Cowan**, N. Vandelli***

* Air Force Institute of Technology, Wright-Patterson AFB, OH 45433
** Air Force Research Laboratory, Wright-Patterson AFB, OH 45433
*** Microcosm Technologies, Inc. Cambridge, MA 02142

ABSTRACT

Due to the unique structure and small scale of Micro-Electro-Mechanical Systems (MEMS), residual stresses during the deposition processes can have a profound affect on the functionality of the MEMS structures. Typically, material properties of thin films used in surface micromachining are not controlled during deposition. The residual stress, for example, tends to vary significantly for different deposition methods. Currently, few techniques are available to measure the residual stress in MEMS devices. In this paper, Raman spectroscopy is utilized to examine the residual and induced stress in a polysilicon MEMS micromirror. Finite element modeling (FEM) curves using MEMCAD software are generated and compared to Raman spectroscopy stress profiles for test validation. As MEMS structures become more complex, the stress images generated from FEM and Raman spectroscopy will provide valuable information on stress fields in the structure.

Keywords: MEMS, Raman Spectroscopy, Residual Stress, MUMPs, Young's Modulus.

1 INTRODUCTION

MEMS systems are becoming an integral part of our everyday lives. MEMS are used in many applications such as air bag triggers in automotive applications and MEMS pressure gauges. However, on the scale on which MEMS devices are built, residual stresses can play a major role in the successful use and reliability of the device. In many devices with free standing structures, residual stress can physically warp the device to a degree that the free standing structure either curls upward or touches the substrate and is no longer useful because of 'stiction' effects. In micromirror arrays, residual stress gradients can destroy the flatness of the mirror surfaces making them unusable. However, if the residual stresses can be mapped, and eventually controlled during the manufacturing processes, the designer will no longer be forced to limit his design to the manufacturing stresses. These stresses will in effect be an additional degree of freedom for the MEMS designer.

Several different methods have been used to characterize strain in thin films of silicon. Interferometric measurements of deflection and curvature yield average strain measurements. X-ray diffraction techniques can measure stress but the technique is cumbersome and lacks a high spatial resolution [1]. Micro-Raman spectroscopy is increasingly being used to measure stress in electronic silicon devices. This technique is nondestructive and accurate for most required stress measurements. Since it is an optical technique, micro-Raman spectroscopy shows promise as a minimally invasive *in situ* measurement technique for the manufacture of MEMS devices.

2 EXPERIMENTAL

In this paper, we investigate the measurement of residual and induced stress in a MEMS micromirror flexure utilizing micro-Raman spectroscopy. Raman spectra were obtained using a Renishaw system 2000 Raman microscope in backscattering mode. The laser used was an Ar^+ laser at 514.5 nm. The laser power was limited to 3.0 mW to minimize sample heating. Scanning was accomplished using a stepping XYZ stage with a 1 μm resolution. The MEMS device used in these experiments was a polysilicon micromirror fabricated using the Cronos Multi-User MEMS Processes, or MUMP's process. The microdevice was wire bonded to a 144-pin grid array (PGA) and mounted on a test fixture. Scans of these structures were accomplished by focusing the laser through a microscope objective, resulting in a spatial resolution of approximately 1 μm. The frequency shifts in the Raman spectra were found by fitting the single Raman peak with a Lorentzian function with an error of approximately 0.1 Rcm^{-1} (The unit 'Rcm^{-1}' denotes "relative cm^{-1}"; the frequency is always measured relative to the frequency of the laser light).

3 THEORY

The goal of this paper is to show that micro-Raman spectroscopy can be used as an effective measurement technique to determine local and induced stress values in MEMS devices. Several papers have shown that micro-Raman spectroscopy is an effective measure of mechanical stress in silicon [1]–[3]. To achieve this goal, the focus is not on the precise value of stress, but rather on demonstrating that the stress profiles obtained from micro-

Raman spectroscopy are both reasonable and helpful to the MEMS designer. However, to fully understand the data presented, it is necessary to briefly develop the relevant theory.

Ganesan [4] was one of the first to show the effects of strain on diamond structured crystals. The Raman spectra of silicon has one peak at 520 Rcm^{-1}, which is comprised of three degenerate $k = 0$ optical phonon modes. Using the following secular equation one can solve for the effect of strain on these optical modes

$$\begin{vmatrix} a & 2r\epsilon_{12} & 2r\epsilon_{13} \\ 2r\epsilon_{12} & b & 2r\epsilon_{23} \\ 2r\epsilon_{13} & 2r\epsilon_{23} & c \end{vmatrix} = 0 \quad (1)$$

where

$$a = p\epsilon_{11} + q(\epsilon_{22} + \epsilon_{33}) - \lambda_1 \quad (2)$$

$$b = p\epsilon_{22} + q(\epsilon_{33} + \epsilon_{11}) - \lambda_2 \quad (3)$$

$$c = p\epsilon_{33} + q(\epsilon_{11} + \epsilon_{22}) - \lambda_3 \quad (4)$$

The constants p, q, and r are the optical phonon deformation potentials, and ϵ_{ij} are the strain tensor components. By solving equation (1) for the eigenvalues, the following equation relates the solutions to the shift in the Raman peak frequencies

$$\lambda_{m(m=1-3)} = \omega_s^2 + \omega_u^2 \quad (5)$$

where ω_s and ω_u are the stressed and unstressed Raman frequencies for the crystal. The strain components ϵ_{ij} are related to the stress components σ_{ij} (Pa) through Hooke's law

$$\begin{bmatrix} \epsilon_{11} \\ \epsilon_{22} \\ \epsilon_{33} \end{bmatrix} = \begin{bmatrix} S_{11} & S_{12} & S_{12} \\ S_{12} & S_{22} & S_{12} \\ S_{12} & S_{12} & S_{33} \end{bmatrix} \begin{bmatrix} \sigma_1 \\ \sigma_2 \\ \sigma_3 \end{bmatrix} (unitless) \quad (6)$$

where [S] (Pa^{-1}) is the elastic compliance matrix for a cubic crystal structure [5]. By assuming uniaxial stress, the following stress/strain relations are obtained from equation (6): $\epsilon_{11} = S_{11}\sigma_1$, $\epsilon_{22} = S_{12}\sigma_2$, and $\epsilon_{33} = S_{12}\sigma_3$. By substituting these stress/strain relationships into equation (1), solving equations (1) and (5), and utilizing the fact that only the third phonon mode will be visible in the backscattering mode from a [100] surface, one obtains

$$\triangle\omega_3 = \frac{\lambda_3}{2\omega_0} = \frac{\sigma}{2\omega_0}[(pS_{12} + q(S_{11} + S_{12})] \quad (7)$$

Using the material parameters found in De Wolf [2], equation (7) reduces to

$$\triangle\omega_3(cm^{-1}) = -2 \times 10^{-9}\sigma(Pa) \quad (8)$$

It can be seen from equation (7) that for the case of uniaxial stress, the Raman shift is linear with the change in stress. The Raman center frequency for unstressed silicon is 520 Rcm^{-1}. Compressive stress will shift this frequency value higher while tensile stress will shift it lower.

In the following set of experiments, there are several possible sources of error to include: 1) the imperfect assumption of uniaxial stress, 2) the use of the phonon deformation potential constants for single crystal silicon rather than phosphorus doped polycrystalline silicon, and 3) our value of Young's modulus. The flexures of the micromirror device were selected since they have high length to deflection ratios (114 $\mu m \times \sim 0.6\ \mu m$). These high ratios ensure the uniaxial stress assumption is reasonable and the resulting stress profiles can qualitatively confirm that stress values were actually being observed. The results presented in the next section provide an approximation of the true stress values present in the MEMs device.

4 RESULTS AND DISCUSSION

Through the use of micro-Raman spectroscopy and finite element models (FEM), the residual and induced stress profiles for the MEMS micromirror flexure can be compared. This allows us to address changes in stress values using various electrostatic actuation voltage levels. Through this observation and comparison of the experimental data to the FEM data, the feasibility and accuracy of using micro-Raman spectroscopy to measure stress can be determined.

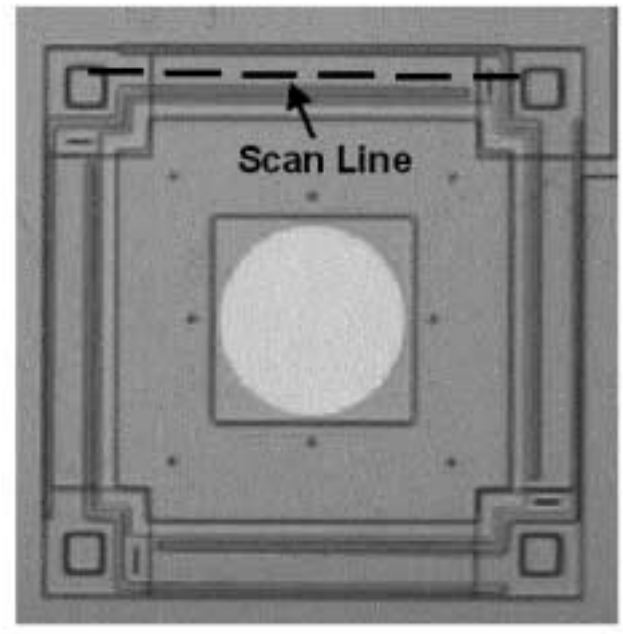

Figure 1: $MUMPs^{TM}$ Polysilicon Micromirror

The MEMS micromirror shown in Figure 1 is a single element of a deformable mirror array for use in adaptive optics [6]. The mirror is actuated electrostatically

through the use of an electrode pad located under the center of the mirror. As part of the MEMS design, dimples located under the flexures prevent 'stiction' effects when snap-down occurs. The flexures surrounding the mirror are constrained from movement by anchors at one end and attached to the mirror at the other end. As seen in Figure 1, the flexure attachment to the mirror is solid. This will allow translation at the end of the flexure, but will resist rotation. The Raman scan line is identified in Figure 1.

The micromirror flexure can be modeled as a beam as shown in Figure 2. As the actuated mirror flexes the beam downward, one would expect to see the induced stress distribution on the top of the beam to be essentially a backward S-shape. A tensile stress section should exist close to the fixed end of the beam followed by an inflection point and a compressive stress near the end attached to the mirror.

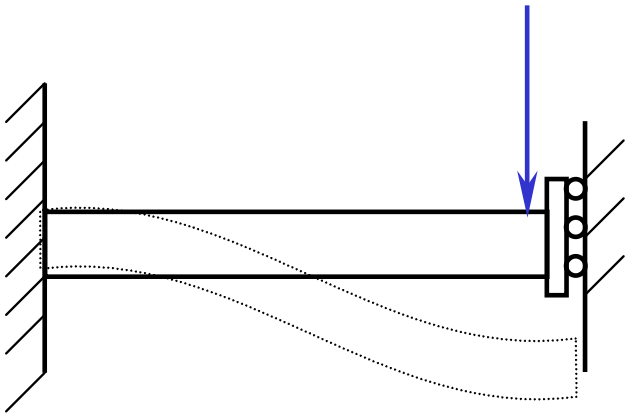

Figure 2: Mechanical Beam Model of the Micromirror Flexure

Raman stress measurements include both induced and residual stresses. To accurately characterize the induced stress, one must first obtain the residual stress. Figure 3 shows both the Raman frequency shift along the longitudinal axis of the flexure as well as the resulting residual stress calculated assuming uniaxial stress. The flat region on the left-hand side of both curves corresponds to the anchor of the flexure. The stress distribution starts with a small tensile stress close to the anchor and reaches a maximum of approximately 900 MPa just past the midpoint of the flexure, then begins to relax as it approaches the mirror attachment. The assumption of uniaxial stress should be fairly reasonable since they have high length to deflection ratios. However, the geometry of the mirror attachment will add some degree of torsion to the flexure.

To induce stress in the micromirror flexure, the micromirror was electrostatically actuated for voltage levels of 10, 13, 16, and 20 V. Since snap-down of the mirror occurs around 16.5 V, these voltage levels will assist

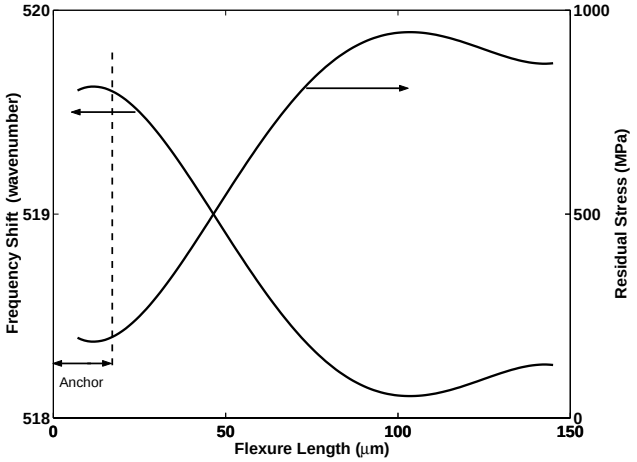

Figure 3: Residual Stress Distribution along the Micromirror Flexure

in identifying the snapdown region of the micromirror using Raman spectroscopy. To avoid hysteresis effects during the actuation, care was taken to approach the voltage value from the lower side for all measurements. At each voltage setting, a Raman line scan was taken across the same physical dimensions used to find the residual stress distribution in Figure 3. The residual stress (the stress measured with no electrostatic actuation) was subtracted from each of the corresponding stress distributions to yield the induced stress curves. In an attempt to verify the induced stress curves obtained experimentally using micro-Raman spectroscopy, a MEMCAD 4.8 finite element model (FEM) was used. In addition, the FEM stress curves will help support the assumption of uniaxial stress in the flexure.

Figure 4 illustrates both the Raman and FEM stress curves for 10, 13, 16 and 20 V applied to the micromirror. The Raman stress profiles depicted are fourth order polynomial fits, and have been adjusted to eliminate the anchor end for ease of comparison to the FEM profile. As can be observed from Figure 4, the stress magnitude is higher in the Raman stress profile. One can account for some of the error due to the residual stress value used in the FEM model. The residual compressive stress value used was 9 MPa. This value is obtained by the MUMPs foundry process through a wafer curvature technique. This technique is used to determine the residual stress for the MUMPs process. The wafer curvature technique provides a mean value of film stress across the wafer. No localized stress information or stress gradients can be obtained using this method. The localized residual stress was later determined to be $\sim$36 MPa using a buckled beam array [7]. This would account for a significant percentage of the error observed.

The FEM stress curve for 20 V (snap-down) is shown in Figure 5. The shape of the induced stress curve in the snap-down region conforms qualitatively to the expected

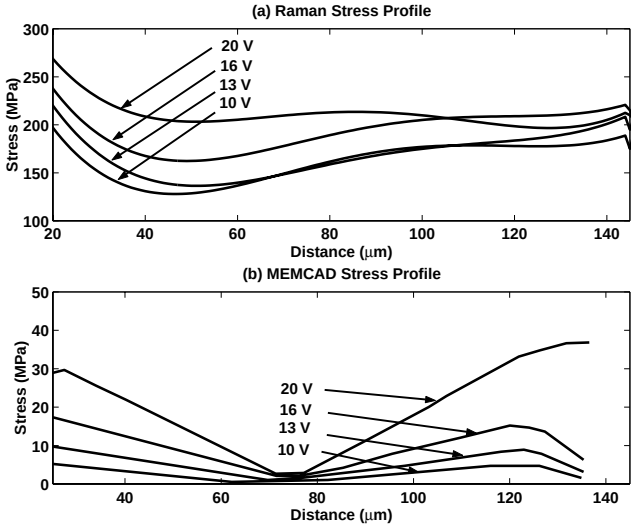

Figure 4: Fourth Order Polynomial Fit of Raman Data vs. MEMCAD FEM Stress Profiles

S-shaped distribution for the beam model shown in Figure 2. In fact, there is tensile stress close to the anchor (left) end of the flexure which decreases through an inflection point. This is followed by an increase in tensile stress near the right end of the beam. The shape of the curves corresponds well with the nature of electrostatic actuation. The shape changes gradually as voltage is increased. Then, as the snap down voltage is approached, the shape of the curve changes abruptly corresponding to a large change in deflection over a short voltage range.

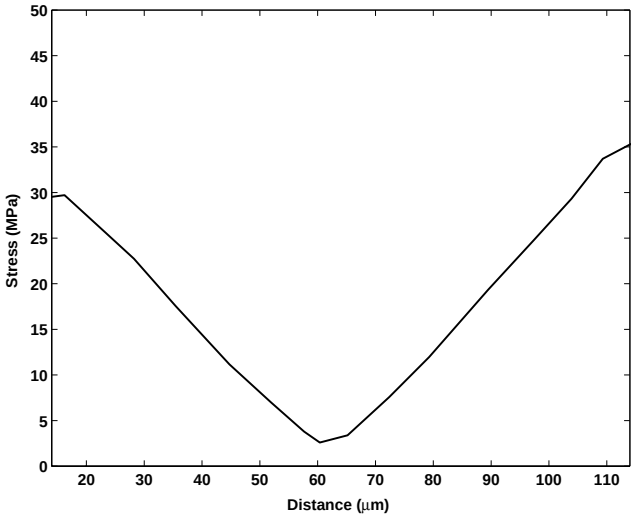

Figure 5: FEM Induced Stress in the Flexure at Snap-down

All stress curves obtained from the Raman data are based on the assumption of uniaxial stress. Based on this assumption, the stress will predominantly occur down the length of the flexure (x-direction). The stress across the flexure (y-direction) and through the depth of the flexure (z-direction) should be minimal. Based on our calculated MEMCAD stress profiles for the y and z-directions, we determined that the magnitude of the stress in the y and z-directions is negligible when compared to the uniaxial FEM result along the length of the flexure. Thus, the modeling results suggest that the uniaxial stress approximation is valid.

5 CONCLUSIONS

In this paper, we demonstrated the feasibility of micro-Raman spectroscopy for measuring both residual and induced stresses in a MEMS device. Future work will focus on increasing the correlation between our model and experimental results. This work was sponsored by the Air Force Research Laboratory.

REFERENCES

[1] E. Anastassakis, A. Pinczuk, E. Burstein, F.H. Pollak, and M. Cardona, "Effect of Static Uniaxial Stress on the Raman Spectrum of Silicon," Solid State Communications, Vol. 8 No. 2, 133-138, 1970.

[2] I. De Wolf, "Micro-Raman spectroscopy to study local mechanical stress in silicon integrated circuits," Semiconductor Science Technology, Vol. 11, 139-154, 1996.

[3] M. Siakavellas, E. Anastassikis, G. Koltsas, and A.G. Nassiopoulos, "Micro-Raman characterization of stress distribution within free standing mono- and poly-crystalline silicon membranes," Microelectronic Engineering Vol. 41/42, 469-472, 1998.

[4] S. Ganesan, A. Maradudin, J. Oitmaa, "A Lattice Theory of Morphic Effects in Crystals of the Diamond Structure," Annals of Physics, Vol. 56, 556-594, 1970.

[5] J.F. Nye, "Physical Properties of Crystals," Oxford Science Publications, Oxford, p 140, 1957.

[6] W. Cowan, "Surface Micromachined Segmented Mirrors for Adaptive Optics," IEEE Journal of Selected Topics in Quantum Electronics, Vol. 8, 90-101, 1999.

[7] W. Fang and J. A. Wickert, "Post buckling of micromachined beams," Journal of Micromachanical Microengineering, Vol. 4, 116-122, 1994.